

Estimation of the Self-similarity Index of Non-stationary Increments Self-similar Processes via Lamperti Transformations

William Wu¹ and Qidi Peng²

¹*Rancho Cucamonga High School, e-mail: wwu49387@gmail.com*

²*Institute of Mathematical Sciences, Claremont Graduate University, e-mail: [*qidi.peng@cgu.edu](mailto:qidi.peng@cgu.edu)*

Abstract: We introduce a novel method for estimating the self-similarity index of a general H -self-similar process with either stationary or non-stationary increments. The estimation algorithm is developed based on a modified Lamperti transformation, which transforms H -self-similar processes to stationary ones. As an application, we show how to use this approach to estimate the self-similarity index of fractional Brownian motion, subfractional Brownian motion, bifractional Brownian motion, and trifractional Brownian motion. Simulation study is performed to support the consistency of our estimators. Implementation in Python is publicly shared. Application on the estimation of the self-similarity index of the Nile river water level data from the year 900 to 1200 C.E..

MSC2020 subject classifications: Primary 60G18, 60G22; secondary 65C10.

Keywords and phrases: Estimation, self-similarity index, Lamperti transformation, subfractional Brownian motion, bifractional Brownian motion, trifractional Brownian motion.

1. Literature Review on the Estimation of the Self-similarity Index

Self-similar processes are stochastic processes that exhibit the property of invariance in distribution under scaling of time and space. These processes are essential notions in stochastic processes and fractal geometry [18], with diverse applications in real-world fields such as packet inter-arrival times and burst lengths [1, 12], and global financial equity markets [3, 4, 15, 17]. Such processes exhibit the phenomenon of “self-similarity” and are often associated with the “rough path” feature: the process’s sample path is mainly characterized by its self-similarity index. In this paper, we consider the H -self-similar process defined below:

Definition 1.1. We say $V = \{V(t)\}_{t \in \mathbb{R}}$ is an H -self-similar process with self-similarity index $H \in (0, 1)$, if

$$\{V(at)\}_{t \in \mathbb{R}} \stackrel{\text{f.d.d.}}{=} \{|a|^H V(t)\}_{t \in \mathbb{R}}, \text{ for any real number } a \neq 0, \quad (1.1)$$

where $\stackrel{\text{f.d.d.}}{=}$ denotes equality in finite dimensional distribution, i.e., for any $n \geq 1$ and any $t_1, \dots, t_n \in \mathbb{R}$,

$$(V(at_1), \dots, V(at_n)) \stackrel{\text{law}}{=} |a|^H (V(t_1), \dots, V(t_n)), \text{ for any real number } a \neq 0.$$

Concerning to estimate the self-similarity index H of a H -self-similar process, there exist several method in the literature, however, each of them deals with a special case. Therefore, the goal of this paper is to remedy this inconvenience by developing a general method to estimate the self-similarity index of a large class of fourth order H -self-similar processes.

2. A Modified Lamperti Transformation: A Novel Estimation Approach

2.1. Lamperti Transformation

Our simulation approaches are inspired by the Lamperti transformations. In 1962, Lamperti introduced the Lamperti transformation to transform H -self-similar processes to stationary processes, and the inverse operator does so vice versa. The two transformations are defined as follows [10].

Definition 2.1. Let $\{V(t)\}_{t \in \mathbb{R}}$ be an H -self-similar process with self-similarity index $H \in (0, 1)$, the Lamperti transformation of $\{V(t)\}_{t \in \mathbb{R}}$ is defined to be

$$\mathcal{L}_V(t) = e^{-tH} V(e^t) \text{ for } t \in \mathbb{R}. \quad (2.1)$$

Let $\{U(t)\}_{t \in \mathbb{R}}$ be a stationary stochastic process, i.e., for any integer $n \geq 1$, any time indices $t_1, \dots, t_n \in \mathbb{R}$ and any time shifting parameter $h > 0$, we have

$$(U_{t_1}, \dots, U_{t_n}) \stackrel{\text{law}}{=} (U_{t_1+h}, \dots, U_{t_n+h}).$$

For each $H \in (0, 1)$, the inverse Lamperti transformation of $\{U(t)\}_{t \in \mathbb{R}}$ is given by

$$\mathcal{L}_U^{-1}(0) = 0; \quad \mathcal{L}_U^{-1}(t) = t^H U(\log t) \text{ for } t > 0.$$

Through the paper, we assume that

$$\sigma^2 = \text{Var}(V(1)). \quad (2.2)$$

The main goal of this paper is to provide a novel and general method to estimate the self-similarity index of $\{V(t)\}_{t \in [0,1]}$. The options of the methodologies depend on the situation for the cases for known σ and unknown σ . In Definition 2.1, the fact that $\{\mathcal{L}_V(t)\}_{t \in \mathbb{R}}$ is stationary inspires us to develop a novel estimation strategy. Heuristically speaking, our method involves first transforming the H -self-similar process to an ergodic stationary one by using some modified Lamperti transformation, then running statistical estimation of the self-similarity index on the latter process.

2.2. Estimation of the Self-similarity Index When σ^2 is Given

If σ^2 is known, we assume that $\{\mathcal{L}_V(t)\}_{t \in [0,1]}$ is ergodic. In view of the definition of H -self-similar process and the Lamperti transformation, we suggest the following way to estimate the self-similarity index H of the process $\{V(t)\}_{t \in [0,1]}$.

Algorithm 2.2.

Step 1 Define the sequences $a = (a_0, \dots, a_n)$ and $b = (b_0, \dots, b_n)$:

$$a = \left(V \left(\frac{\lfloor n^{j/n} \rfloor}{n} \right) \right)_{j=0, \dots, n} \quad \text{and} \quad b = \left(n^{1-j/n} \right)_{j=0, \dots, n}, \quad (2.3)$$

where $\lfloor \bullet \rfloor$ denotes the floor number.

Step 2 Use a non-linear least squares method to solve H from the equation

$$f_n(H) := \frac{\sum_{j=0}^n a_j^2 b_j^{2H}}{n+1} - \sigma^2 = 0. \quad (2.4)$$

For example, the solution \widehat{H} can be solved from Halley's method [19].

Let us heuristically explain the rationales of Algorithm 2.2.

1. In **Step 1**, it is from the integer $J_n = \lceil -n \log_n(n^{1/n} - 1) \rceil$ such that $\{\lfloor n^{j/n} \rfloor\}_{j \in \{0, \dots, n\}}$ are all distinct. In fact, J_n is the smallest integer such that

$$n^{(j+1)/n} - n^{j/n} \geq 1 \quad \text{for all } j \geq J_n.$$

2. In **Step 2**, we have used the fact that

$$U_n \left(\frac{j}{n} \right) := \mathcal{L}_V \left(\left(\frac{j}{n} - 1 \right) \log(n) \right) = n^{-H(j/n-1)} V(n^{j/n-1}) \quad \text{for } j \in \{0, \dots, n\} \quad (2.5)$$

is stationary and ergodic. Therefore,

$$\frac{\sum_{j=0}^n V(n^{j/n-1})^2 n^{2H(1-j/n)}}{n+1} - \text{Var}(V(1)) \xrightarrow[n \rightarrow +\infty]{\mathbb{P}} 0. \quad (2.6)$$

We also have

$$V \left(n^{j/n-1} \right) \approx V \left(\frac{\lfloor n^{j/n} \rfloor}{n} \right) = a_j \quad \text{a.s..}$$

It results that

$$\frac{\sum_{j=0}^n a_j^2 b_j^{2H}}{n+1} - \sigma^2 \xrightarrow[n \rightarrow +\infty]{\mathbb{P}} 0. \quad (2.7)$$

2.3. Estimation of the Self-similarity Index When σ^2 is Unknown

If σ^2 is unknown, we further assume that $\mathbb{E}(V(1)^4) < +\infty$. We then observe that

$$\hat{\kappa}_n(H) := \frac{(n+1) \sum_{j=0}^n a_j^4 b_j^{4H}}{\left(\sum_{j=0}^n a_j^2 b_j^{2H}\right)^2} \xrightarrow[n \rightarrow +\infty]{\text{a.s.}} \frac{\mathbb{E}(V(1)^4)}{(\mathbb{E}(V(1)^2))^2}.$$

$\hat{\kappa}_n(H)$ is then a consistent estimator of the kurtosis of the stationary distribution $V(1)$. This kurtosis is the measure of dispersion of Z^2 around its expectation 1, where $Z = V(1)^2 / \sqrt{\mathbb{E}(V(1)^2)}$. Therefore, the maximum likelihood estimation method is equivalent to minimizing the kurtosis via H , i.e.,

$$\hat{H}_n := \arg \min_{H \in (0,1)} \hat{\kappa}_n(H) \xrightarrow[n \rightarrow +\infty]{\text{a.s.}} H.$$

We then propose the following algorithm:

Algorithm 2.3.

Step 1 Define the sequences $a = (a_0, \dots, a_n)$ and $b = (b_0, \dots, b_n)$ as in (2.3).

Step 2 Use Brent's method [6] to solve the following optimization problems

$$\hat{H}_n = \arg \min_{H \in (0,1)} \frac{\sum_{j=0}^n a_j^4 b_j^{4H}}{\left(\sum_{j=0}^n a_j^2 b_j^{2H}\right)^2}. \quad (2.8)$$

3. Estimation of the Self-similarity Index with Examples

In this section, we will estimate and the self-similarity index for fractional Brownian motion, subfractional Brownian motion, bifractional Brownian motion, and trifractional Brownian motion.

3.1. Fractional Brownian motion

The fractional Brownian motion $\{B^H(t)\}_{t \geq 0}$ [14] with the Hurst parameter $H \in (0, 1)$ that we consider in this framework is defined as a zero mean Gaussian process with $B^H(0) = 0$ a.s. and covariance function given by: for $s, t \geq 0$,

$$\gamma_{B^H}(s, t) = \frac{\sigma^2}{2} (|t|^{2H} + |s|^{2H} - |t - s|^{2H}). \quad (3.1)$$

In a simulation study, we use our estimation for processes simulated using Wood Chan's method [20]. Simulations and estimations were performed. We generate 200 trajectories of fBm with length $N = 2^l$ for $l \in \{7, 8, 9, 10\}$ and $H \in \{0.2, 0.5, 0.7, 0.8\}$. All of the following results show the mean estimated H and the mean squared error in parentheses. S

TABLE 1
Estimator of H with MSE based on fBm simulated by Wood-Chan's Method: $\sigma^2 = 1$

H	$N = 128$	$N = 256$	$N = 512$	$N = 1024$
0.2	0.237 (0.0213)	0.226 (0.0191)	0.220 (0.0121)	0.209 (0.0084)
0.5	0.538 (0.0524)	0.505 (0.0195)	0.508 (0.0149)	0.510 (0.0112)
0.7	0.733 (0.0715)	0.686 (0.0502)	0.715 (0.0211)	0.715 (0.0125)
0.8	0.823 (0.0916)	0.849 (0.0361)	0.809 (0.0238)	0.818 (0.0219)

The following results are for Algorithm 2.3 where the self-similar scaling parameter is not known.

TABLE 2
Estimator of H with MSE based on fBm simulated by Wood-Chan's Method: σ^2 is unknown

H	$N = 128$	$N = 256$	$N = 512$	$N = 1024$	$N = 8192$
0.2	0.286 (0.0405)	0.264 (0.0307)	0.235 (0.0205)	0.228 (0.0112)	0.219 (0.0067)
0.5	0.504 (0.0503)	0.504 (0.0311)	0.496 (0.0234)	0.515 (0.0203)	0.507 (0.0105)
0.7	0.668 (0.0350)	0.684 (0.0317)	0.683 (0.0255)	0.658 (0.0253)	0.691 (0.0113)
0.8	0.743 (0.0401)	0.721 (0.0466)	0.754 (0.0276)	0.753 (0.0245)	0.773 (0.0148)

For comparison, we can test the accuracy against the quadratic variation estimation method (QV estimator) [7] and the complex variation estimation method [9] by running the same simulations. The results are given below.

TABLE 3
Quadratic Variation Estimator of H .

H	$N = 128$	$N = 256$	$N = 512$	$N = 1024$
0.2	0.193 (0.0056)	0.204 (0.0025)	0.207 (0.0012)	0.199 (0.0006)
0.5	0.499 (0.0072)	0.498 (0.0030)	0.499 (0.0015)	0.497 (0.0009)
0.7	0.683 (0.0080)	0.690 (0.0036)	0.702 (0.0021)	0.698 (0.0009)
0.8	0.794 (0.0088)	0.799 (0.0044)	0.797 (0.0020)	0.794 (0.0010)

TABLE 4
Complex Variations Estimator of H .

H	$N = 128$	$N = 256$	$N = 512$
0.5	0.500 (0.050)	0.500 (0.022)	0.490 (0.012)
0.7	0.680 (0.040)	0.690 (0.023)	0.710 (0.010)
0.8	0.825 (0.037)	0.805 (0.020)	0.800 (0.008)

The comparison shows that our estimation methods are competitive to the literature ones for estimating the Hurst parameter of fractional Brownian motion.

Additional visualization of the error analysis result is given below.

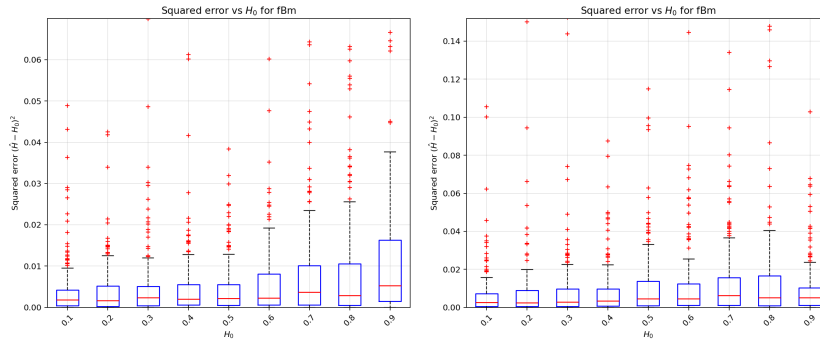


FIG 1. The results are given by left: Algorithm 2.2, right: Algorithm 2.3. Each H_0 consists of 200 simulated paths of length $N = 4096$. Squared error of the estimated parameter is computed for each path and drawn into a boxplot. Outliers over 99th percentile are cut out for the sake of clear visuals.

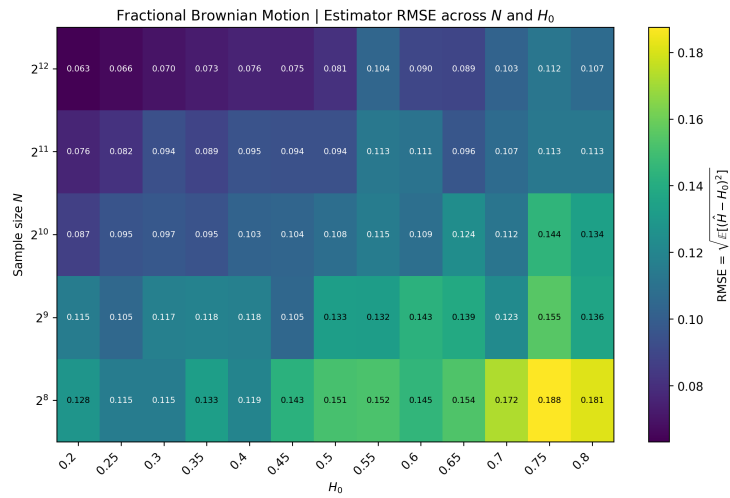


FIG 2. 200 paths of fBm are simulated for each corresponding H_0 and N value with the RMSE plotted as a heatmap distribution. The results show empirical convergence towards 0 as the path length increases and H_0 value decreases.

The above figures show that in both cases, the overall performance of the estimation is consistent.

3.2. Subfractional Brownian motion

The subfractional Brownian motion $\{S^H(t)\}_{t \geq 0}$ is defined to be a zero-mean Gaussian process with $S^H(0) = 0$ a.s. and covariance function (see [5]):

$s, t \geq 0$,

$$\text{Cov}(S^H(t), S^H(s)) = \sigma^2 \left(t^{2H} + s^{2H} - \frac{1}{2} \{(t+s)^{2H} + |t-s|^{2H}\} \right), \quad (3.2)$$

where the parameter $H \in (0, 1)$. By (3.2), we know that $\{S^H\}_{t \geq 0}$ is an H -self-similar process. However, unlike the fractional Brownian motion, the subfractional Brownian motion has non-stationary increments when $H \neq 1/2$. This property makes its simulation quite challenging. The simulation approach existing in the literature is based on the DPW method provided in [16] with available code in <https://pypi.org/project/fractal-analysis/>.

To estimate H when σ^2 is known as 1, it suffices to note that

$$\sigma^2 = \text{Var}(S^H(1)) = 2 - 2^{2H-1}.$$

Modifying a bit Algorithm 2.2, we obtain the algorithm to estimate H .

Algorithm 3.1. Let $(S^H(j/n))_{j=1, \dots, n}$ be an observed sample path of $\{S^H(t)\}_{t \in [0, 1]}$ with covariance function γ_{S^H} with $\sigma^2 = 1$.

Step 1 Let the sequences $a = (a_0, \dots, a_n)$ and $b = (b_0, \dots, b_n)$:

$$a = \left(S^H \left(\frac{\lfloor n^{j/n} \rfloor}{n} \right) \right)_{j=0, \dots, n} \quad \text{and} \quad b = \left(n^{1-j/n} \right)_{j=0, \dots, n},$$

where $\lfloor \bullet \rfloor$ denotes the floor number.

Step 2 Use a non-linear least squares method to solve H from the equations

$$f_n(H) := \frac{\sum_{j=0}^n a_j^2 b_j^{2H}}{n+1} - (2 - 2^{2H-1}) = 0.$$

We show that our estimation methods perform well for sfBm using the DPW simulation algorithm. We generate 200 trajectories of sfBm with length $N = 2^l$ for $l \in \{7, 8, 9, 10\}$ and $H \in \{0.2, 0.5, 0.7, 0.8\}$. The following results show the mean estimator H with the MSE in parentheses.

TABLE 5
Subfractional Brownian motion: Algorithm 3.1

H	$N = 128$	$N = 256$	$N = 512$	$N = 1024$
0.2	0.228 (0.0218)	0.216 (0.0128)	0.228 (0.0090)	0.214 (0.0071)
0.5	0.509 (0.0142)	0.509 (0.0107)	0.508 (0.0077)	0.508 (0.0060)
0.7	0.695 (0.0081)	0.703 (0.0066)	0.702 (0.0052)	0.705 (0.0044)
0.8	0.785 (0.0061)	0.799 (0.0051)	0.799 (0.0033)	0.801 (0.0027)

The simulation results for algorithm 2.3 is given below:

TABLE 6
Subfractional Brownian motion: Algorithm 2.3

H	$N = 128$	$N = 256$	$N = 512$	$N = 1024$	$N = 8192$
0.2	0.251 (0.0370)	0.266 (0.0272)	0.250 (0.0274)	0.247 (0.0191)	0.220 (0.0086)
0.5	0.500 (0.0388)	0.501 (0.0293)	0.516 (0.0227)	0.500 (0.0153)	0.500 (0.0096)
0.7	0.635 (0.0494)	0.657 (0.0273)	0.661 (0.0263)	0.668 (0.0240)	0.680 (0.0109)
0.8	0.750 (0.0351)	0.761 (0.0314)	0.762 (0.0268)	0.732 (0.0291)	0.762 (0.0171)

Additional data visualization is given.

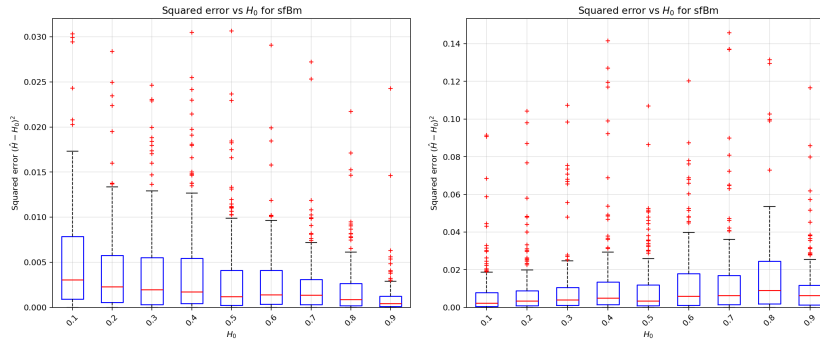


FIG 3. The results are given by left: Algorithm 2.2, right: Algorithm 2.3. Each H_0 consists of 200 simulated paths of length $N = 4096$. Squared error of the estimated parameter is computed for each path and drawn into a boxplot. Outliers over 99th percentile are cut out for the sake of clear visuals.

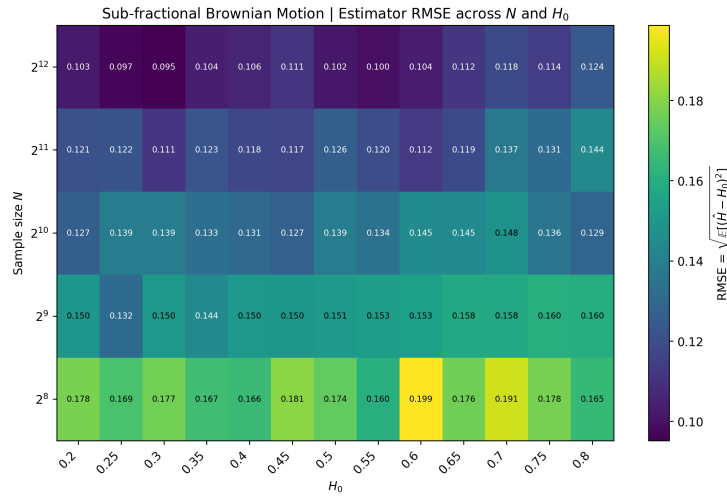


FIG 4. 200 paths of sfBm are simulated for each corresponding H_0 and N value with the RMSE plotted as a heatmap distribution. The results show empirical convergence towards 0 as the path length increases.

3.3. Bifractional Brownian motion

The bifractional Brownian motion $\{B^{H,K}(t)\}_{t \geq 0}$ is a zero-mean Gaussian process with $B^{H,K}(0) = 0$ a.s. and covariance function (see [8]): for $s, t \geq 0$,

$$\text{Cov}(B^{H,K}(t), B^{H,K}(s)) = \frac{\sigma^2}{2K} \{(t^{2H} + s^{2H})K - |t - s|^{2HK}\}, \quad (3.3)$$

where the parameters $H \in (0, 1)$ and $K \in (0, 1]$. By (3.3), we see that $\{B^{H,K}(t)\}_{t \geq 0}$ is an HK -self-similar process. When $K = 1$, $\{B^{H,1}(t)\}_{t \geq 0}$ becomes a fractional Brownian motion with the Hurst parameter H . For $K < 1$, the bifractional Brownian motion does not have stationary increments. To estimate the self-similarity HK , it suffices to apply Algorithm 2.2 and Algorithm 2.3. Note that the simulation method is also provided in the DPW method [16].

The following table shows our estimation method for bfBm using the DPW simulation algorithm. Like before, we will generate 200 trajectories of bfBm with lengths $N = 128, 256, 512, 1024$. This will be tested on paths with $(H, K) \in (\{0.2, 0.8\}, \{0.5, 0.8\})$ to estimate the self-similarity value HK .

TABLE 7
Bifractional Brownian motion: Algorithm 2.2 with $\sigma^2 = 1$

(H, K)	$N = 128$	$N = 256$	$N = 512$	$N = 1024$
(0.2, 0.5)	0.108 (0.0074)	0.107 (0.0058)	0.114 (0.0044)	0.111 (0.0026)
(0.2, 0.8)	0.174 (0.0207)	0.172 (0.0106)	0.172 (0.0072)	0.175 (0.0051)
(0.8, 0.5)	0.391 (0.0131)	0.418 (0.0124)	0.399 (0.0075)	0.404 (0.0042)
(0.8, 0.8)	0.650 (0.0344)	0.654 (0.0186)	0.635 (0.0151)	0.654 (0.0079)

The results for Algorithm 2.3 when the scaling parameter is not known is given below.

TABLE 8
Bifractional Brownian motion: Algorithm 2.3 with unknown σ^2

(H, K)	$N = 128$	$N = 256$	$N = 512$	$N = 1024$	$N = 8192$
(0.2, 0.5)	0.230 (0.0627)	0.200 (0.0428)	0.161 (0.0192)	0.149 (0.0139)	0.122 (0.0058)
(0.8, 0.5)	0.431 (0.0280)	0.422 (0.0301)	0.417 (0.0196)	0.411 (0.0130)	0.411 (0.0070)
(0.2, 0.8)	0.266 (0.0558)	0.235 (0.0332)	0.212 (0.0200)	0.199 (0.0112)	0.186 (0.0081)
(0.8, 0.8)	0.639 (0.0317)	0.616 (0.0287)	0.625 (0.0245)	0.607 (0.0174)	0.619 (0.0094)

Like before, the data visualization is given.

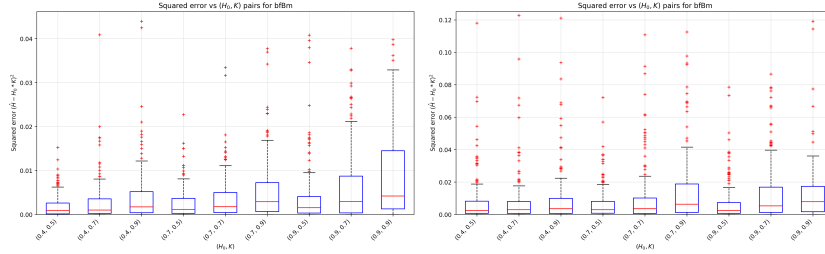


FIG 5. The results are given by left: Algorithm 2.2, right: Algorithm 2.3. Each H_0 consists of 200 simulated paths of length $N = 4096$. Squared error of the estimated parameter is computed for each path and drawn into a boxplot. Outliers over 99th percentile are cut out for the sake of clear visuals.

3.4. Trifractional Brownian Motion

Another example of Gaussian processes with non-stationary increments is the trifractional Brownian motion $\{\tilde{B}^{H,K}(t)\}_{t \geq 0}$ [13]. It is a zero-mean Gaussian process with $\tilde{B}^{H,K}(0) = 0$ a.s. and covariance function: for $s, t \geq 0$,

$$\text{Cov}(\tilde{B}^{H,K}(t), \tilde{B}^{H,K}(s)) = \sigma^2 (t^{2HK} + s^{2HK} - (t^{2H} + s^{2H})^K), \quad (3.4)$$

where the parameters $H \in (0, 1)$ and $K \in (0, 1)$. From its definition, we see that $\{\tilde{B}^{H,K}(t)\}_{t \geq 0}$ is HK -self-similar, and its increment processes are not stationary. Like the bifractional Brownian motion, this process also cannot be simulated using the sum of stationary increments. So far as we know, the only simulation approach suggested in the literature is the DPW method. When $\sigma^2 = 1$, the estimation of the self-similarity index HK is then obtained by a slight modification of Algorithm 2.2:

Algorithm 3.2. Let $(\tilde{B}^{H,K}(j/n))_{j=1, \dots, n}$ be an observed sample path of $\{\tilde{B}^{H,K}(t)\}_{t \in [0,1]}$ with covariance function $\gamma_{\tilde{B}^{H,K}}$.

Step 1 Let the sequences $a = (a_0, \dots, a_n)$ and $b = (b_0, \dots, b_n)$:

$$a = \left(\tilde{B}^{H,K} \left(\frac{\lfloor n^{j/n} \rfloor}{n} \right) \right)_{j=0, \dots, n} \quad \text{and} \quad b = \left(n^{1-j/n} \right)_{j=0, \dots, n},$$

where $\lfloor \bullet \rfloor$ denotes the floor number.

Step 2 Use a non-linear least squares method to solve H, K from the equations

$$f_n(H, K) := \frac{\sum_{j=0}^n a_j^2 b_j^{2HK}}{n+1} - (2 - 2^K) = 0.$$

Like bifractional Brownian motion, the same parameters for testing are applied to tfBm simulated by the DPW algorithm. The results are given below:

TABLE 9
Trifractional Brownian motion: Algorithm 3.2.

(H, K)	$N = 128$	$N = 256$	$N = 512$	$N = 1024$
(0.2, 0.5)	0.203 (0.1038)	0.161 (0.0700)	0.170 (0.0549)	0.171 (0.0442)
(0.2, 0.8)	0.263 (0.0904)	0.263 (0.0603)	0.212 (0.0555)	0.212 (0.0312)
(0.8, 0.5)	0.442 (0.0672)	0.461 (0.0460)	0.427 (0.0319)	0.448 (0.0195)
(0.8, 0.8)	0.659 (0.0520)	0.655 (0.0327)	0.549 (0.0293)	0.656 (0.0188)

Finally the results for trifractional Brownian motion when the scaling parameter is not known, given by Algorithm 2.3, is given below.

TABLE 10
Trifractional Brownian motion: Algorithm 2.3

(H, K)	$N = 128$	$N = 256$	$N = 512$	$N = 1024$	$N = 8192$
(0.2, 0.5)	0.134 (0.0194)	0.140 (0.0210)	0.136 (0.0236)	0.130 (0.0163)	0.121 (0.0094)
(0.8, 0.5)	0.384 (0.0414)	0.421 (0.0375)	0.408 (0.0399)	0.406 (0.0303)	0.405 (0.0185)
(0.2, 0.8)	0.212 (0.0367)	0.182 (0.0220)	0.193 (0.0218)	0.179 (0.0173)	0.172 (0.0144)
(0.8, 0.8)	0.616 (0.0434)	0.626 (0.0379)	0.628 (0.0412)	0.642 (0.0299)	0.628 (0.0194)

The error analysis result is illustrated below:

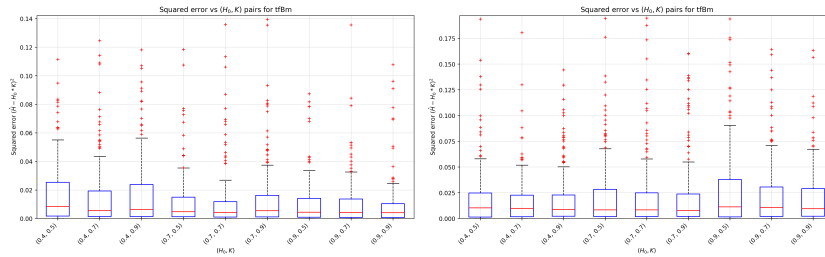


FIG 6. The results are given by left: Algorithm 2.2, right: Algorithm 2.3. Each H_0 consists of 200 simulated paths of length $N = 4096$. Squared error of the estimated parameter is computed for each path and drawn into a boxplot. Outliers over 99th percentile are cut out for the sake of clear visuals.

We conclude that:

- (1) Our estimation method is competitive to the literature ones for estimation of the Hurst parameter of fractional Brownian motion.
- (2) Our estimation fills the gaps when the target process has non-stationary increments. This makes our method be able to estimate the self-similarity indexes of sub-fBm, bifBm, and trifBm.

3.5. Code availability

In this section, we list the codes for all methods mentioned in this paper. Among them, we have contributed the following:

- Estimation process to obtain comparison data (Python): <https://github.com/william11074/Self-similar-Statistical-Inference>
- Simulation algorithm for fBm, sfBm, bfBm, and tfBm using both Wood Chan's method and DPW method, along with implementation of the QV method: pip install fractal-analysis:
<https://pypi.org/project/fractal-analysis/>

4. Real World Application: The Nile River

Studies conducted by Bardet [2] and Lee et. al [11] show that the annual minimum water levels of the Nile River are self-similar with the property of long-range dependency. These papers detail that the self-similarity index of the observed water levels between years 722 and 1281 match $H \approx 0.88$.

We take the interval from the year 900 to 1200 for the Nile River data and using Algorithm 2.3, we get a predicted H value of 0.8545. However, applying parametric bootstrap bias correction, the corrected value $H_{BC} = 0.8790$, matching the results in literature. Open source data is used from <http://lib.stat.cmu.edu/S/beran>.

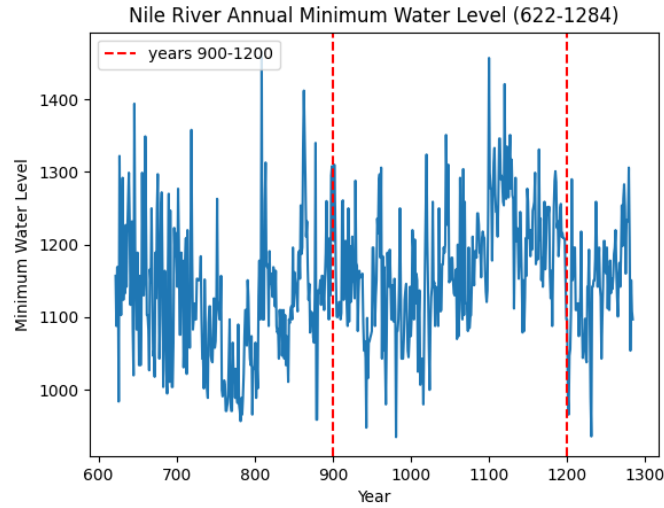


FIG 7. Plotted is the available dataset of annual Nile River data from years 622-1284 C.E. The years 900-1200 is chosen for the estimation of the self-similarity index.

5. Conclusion

This paper develops a general way to estimate the self-similarity index for a given second-order self-similar stochastic process that is ergodic with emphasis that the method works for non-stationary increments self-similar processes. Two estimation algorithms are given for when the scaling parameter is known or unknown. Simulation and testing show that results are accurate and comparable to other methods in the literature. In addition, application to real-world data, the Nile River's historical water level, shows use cases. GitHub code is documented and provided for the estimation algorithms.

References

- [1] ABRY, P., FLANDRIN, P., TAQQU, M. S. and VEITCH, D. (2000). Wavelets for the analysis, estimation, and synthesis of scaling data. *Self-similar Network Traffic and Performance Evaluation* 39–88.
- [2] BARDET, J.-M. (2000). Testing for the presence of self-similarity of Gaussian time series having stationary increments. *Journal of Time Series Analysis* **21** 497–515.
- [3] BIANCHI, S., PANTANELLA, A. and PIANESE, A. (2012). Modeling and simulation of currency exchange rates using multifractional process with random exponent. *International Journal of Modeling and Optimization* **2** 309.

- [4] BIANCHI, S. and PIANESE, A. (2008). Multifractional properties of stock indices decomposed by filtering their pointwise Hölder regularity. *International Journal of Theoretical and Applied Finance* **11** 567–595.
- [5] BOJDECKI, T., GOROSTIZA, L. G. and TALARCZYK, A. (2004). Sub-fractional Brownian motion and its relation to occupation times. *Statistics & Probability Letters* **69** 405–419.
- [6] BRENT, R. P. (1971). An algorithm with guaranteed convergence for finding a zero of a function. *The computer journal* **14** 422–425.
- [7] COEURJOLLY, J.-F. (2005). Identification of multifractional Brownian motion. *Bernoulli* **11** 987–1008.
- [8] HOUDRÉ, C. and VILLA, J. (2003). An example of infinite dimensional quasi-helix. *Contemporary Mathematics* **336** 195–202.
- [9] ISTAS, J. (2012). Estimating self-similarity through complex variations. *Electronic Journal of Statistics* **6** 1392–1408.
- [10] LAMPERTI, J. (1962). Semi-stable stochastic processes. *Transactions of the American Mathematical Society* **104** 62–78.
- [11] LEE, M., GENTON, M. G. and JUN, M. (2016). Testing self-similarity through Lamperti transformations. *Journal of agricultural, biological, and environmental statistics* **21** 426–447.
- [12] LELAND, W. E., TAQQU, M. S., WILLINGER, W. and WILSON, D. V. (1994). On the self-similar nature of Ethernet traffic (extended version). *IEEE/ACM Transactions on Networking* **2** 1–15.
- [13] MA, C. (2013). The Schoenberg–Leévy kernel and relationships among fractional Brownian motion, bifractional Brownian motion, and others. *Theory of Probability & its Applications* **57** 619–632.
- [14] MANDELBROT, B. and VAN NESS, J. W. (1968). Fractional Brownian motions, fractional noises and applications. *SIAM Review* **10** 422–437.
- [15] PENG, Q. (2011). Inférence statistique pour des processus multifractionnaires cachés dans un cadre de modèles à volatilité stochastique, PhD thesis, PhD thesis, Université des Sciences et Technologies de Lille.
- [16] PENG, Q. and WU, W. (2025). Investigation and Development of the Methodologies for Simulating Self-similar Processes. *arXiv preprint arXiv:2512.07296*.
- [17] PENG, Q. and ZHAO, R. (2019). A general class of multifractional processes and stock price informativeness. *Chaos, Solitons & Fractals* **115** 248–267.
- [18] SAMORODNITSKY, G. and TAQQU, M. S. (1994). *Stable Non-Gaussian Random Processes: Stochastic Models with Infinite Variance*. Chapman & Hall, New York.
- [19] SCAVO, T. R. and THOO, J. B. (1995). On the Geometry of Halley’s Method. *The American Mathematical Monthly* **102** 417–426.
- [20] WOOD, A. T. A. and CHAN, G. (1994). Simulation of stationary Gaussian processes in $[0, 1]^d$. *Journal of Computational and Graphical Statistics* **3** 409–432.